JOURNAL OF MATERIALS SCIENCE 33 (1998) 1233–1237

The mechanical properties and microstructure of SiC–AlN particulate composite

YU-BAI PAN, JIAN-HUI QIU, MIKIO MORITA
Faculty of Engineering, Toyama Prefectural University, 5180 Kurokawa, Kosugi, Toyama 939-03, Japan

SHOU-HONG TAN, DONGLIANG JIANG
Shanghai Institute of Ceramics, Chinese Academy, 1295 Rd, Shanghai 20050, People's Republic of China

Silicon carbide (SiC) and aluminium nitride (AlN) were found to form a solid solution at temperatures above 1800 °C. Based on this interesting result, the composite was fabricated by mechanical mixing of the SiC and AlN powders, and hot pressed under 40 MPa at 1950 °C in an argon atmosphere. The objective was to achieve full density and minimize solid solution formation. During the sintering process, the SiC–AlN system passed through three steps to form the solid solution at the end. First, the AlN particle is vaporized from its surface; next, the evaporated AlN is deposited on the surface of the SiC grains and the AlN particle, accompanied by a reduction in its size, and finally, partial SiC and AlN solid-solution formation on the boundary of the SiC grains. Because of the AlN deposition and solid-solution formation at the boundary of SiC grains, a barrier layer was present on the surface of SiC grains. This leads to the formation of fine grains. The toughening mechanism is thought to be by thermal residual stresses, due to the difference between the coefficients of thermal expansion of the matrix SiC and that of the dispersed AlN particles, and crack deflection around the SiC grains. Therefore, it is that which improves the mechanical properties of the SiC–AlN composite. © *1998 Chapman & Hall*

1. Introduction

Several theories have been developed in an attempt to quantify the toughening effect of the addition of second phase particles to a ceramic matrix. Thermal residual stresses arise because coefficient of thermal expansion of the particles is greater than that of the matrix. Other mechanisms that may also operate as a result of the addition of a particulate reinforcement, are crack-front pinning and bowing, crack deflection around particles, crack branching and micro-cracking. At present, the study of composite materials has attracted wide attention.

Silicon carbide (SiC) materials show excellent wear and oxidization resistance at high temperature, but lack the toughness necessary for sufficient reliability. For wide application of SiC ceramic, it is very important to improve its toughness. Many successful studies on the improvement of the mechanical properties of the SiC composites, by second-phase particles, have been reported. For example, SiC–TiC, SiC–Al_2O_3, SiC–TiB_2, etc., were researched. Culter and Miller [1] found that the 2H polymorphs of SiC and AlN can form extensive solid solution at temperatures ranging from 1800–2100 °C, and exhibit analogous lattice parameters. These two materials have more recently been combined as a potential composite material. Much research has been conducted into the formation SiC–AlN mixture powder by organometallic precursors [2], carbonthermal reduction [3], the phase diagrams [4] and fabrication methods [5]. Some properties of SiC and AlN are shown in Table I.

The main purpose of this work was to study the microstructure and thus its effect on reinforcing and toughening the SiC–AlN composite ceramic.

2. Experimental procedure

Composites of a matrix and dispersed particles have interfaces and thus matching problems. The choice of individual components in order to make a composite material, depends on their properties such as crystallographic, electronic, mechanical, thermodynamics and thermomechanics. The SiC–AlN system was selected to fabricate the composite in the present study.

AlN, with an average particle size of 3 μm, was used as reinforcing and toughening particles. Powder of monolithic α-SiC of 0.6 μm was mixed with AlN and Y_2O_3 by ball milling for 10 h. The composition SiC:AlN:Y_2O_3 (weight ratio) was 85:14.5:0.5, in which the Y_2O_3 was added as a sintering aid. The shapes of the SiC and AlN powders are shown in Fig. 1.

TABLE I Some physical properties of SiC and AlN

Materials and properties	SiC	AlN
Density (g/cm^{-3})	3.21	3.26
Crystal structure	Hexagonal	Hexagonal
Lattice constant (nm)	$a_0 = 0.30763$, $c_0 = 0.50480$	$a_0 = 0.31114$, $c_0 = 0.49792$
Thermal expansion coefficient ($10^{-6}K^{-1}$)	4.5	6.09
Young's modulus (GPa)	410	350
Thermal conductivity ($W\,m^{-1}\,K^{-1}$)	54.43	30.10
Bending strength (MPa)	450 (boron, carbon add.)	200–400
Fracture toughness ($MPa\,m^{1/2}$)	4–4.0 (boron, carbon add.)	2

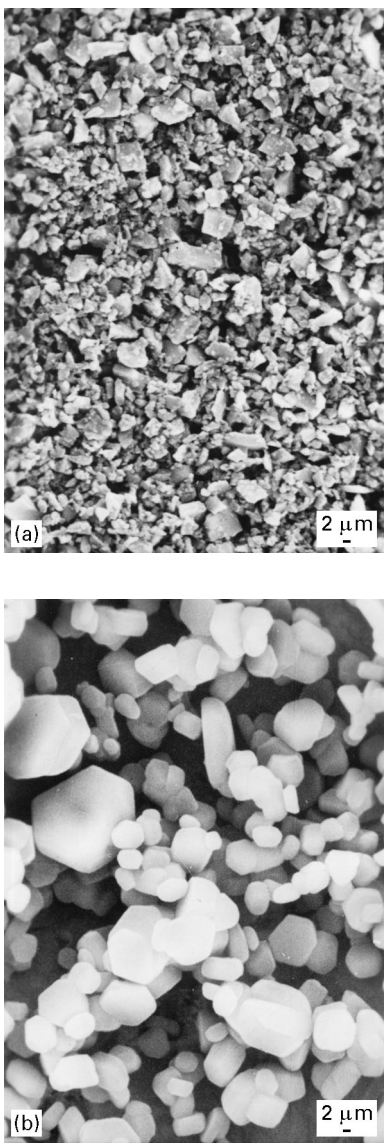

Figure 1 The shape of (a) SiC and (b) AlN powders.

Then the mixture of α-SiC, AlN and Y_2O_3 powders was hot pressed in graphite dies. Through sintering under 40 MPa pressure at 1950 °C in an argon atmosphere, the dense SiC–AlN composite material was obtained.

The strength at room temperature and 1400 °C was measured by a three-point bending test with a specimen size of $3T \times 4W \times 36L\,mm^3$. The test was conducted using an Instron materials testing machine, and the deformation rate was $0.5\,mm/min^{-1}$. The fracture toughness of the materials was evaluated using specimens tested in indentation strength-in-bending (ISB).

The microstructures of the cracks and the boundary interface of the SiC–AlN composite material were observed by energy dispersive X-ray spectroscopy (EDXS), scanning electron microscopy (SEM) and transmission electron microscopy (TEM).

3. Results and discussion

3.1. Microstructure

Through SEM observation, the fracture surface of the bent bar specimen is seen to have an unruly structure showing numerous rising and falling peaks, as shown in Fig. 2. The AlN is well-distributed in the microstructure of the composite material, as seen through aluminum element detection by EDXS in the SEM. At the same time, the microstructure in this composite has fine grains, the average size of which is about 1 μm. The microstructure seen by TEM observation is shown in Fig. 3.

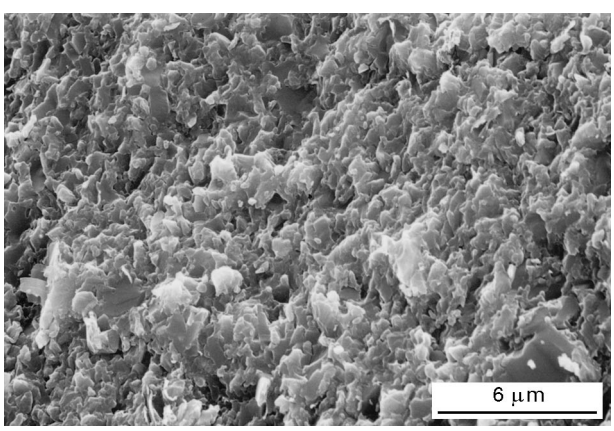

Figure 2 Scanning electron micrograph of the fracture surface of SiC–AlN.

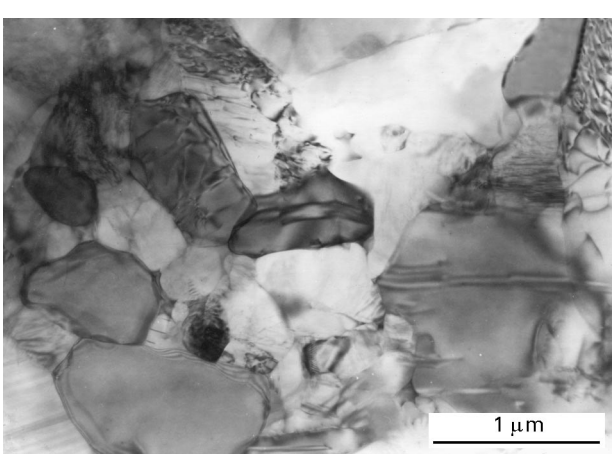

Figure 3 Transmission electron micrograph of the microstructure of SiC–AlN composite.

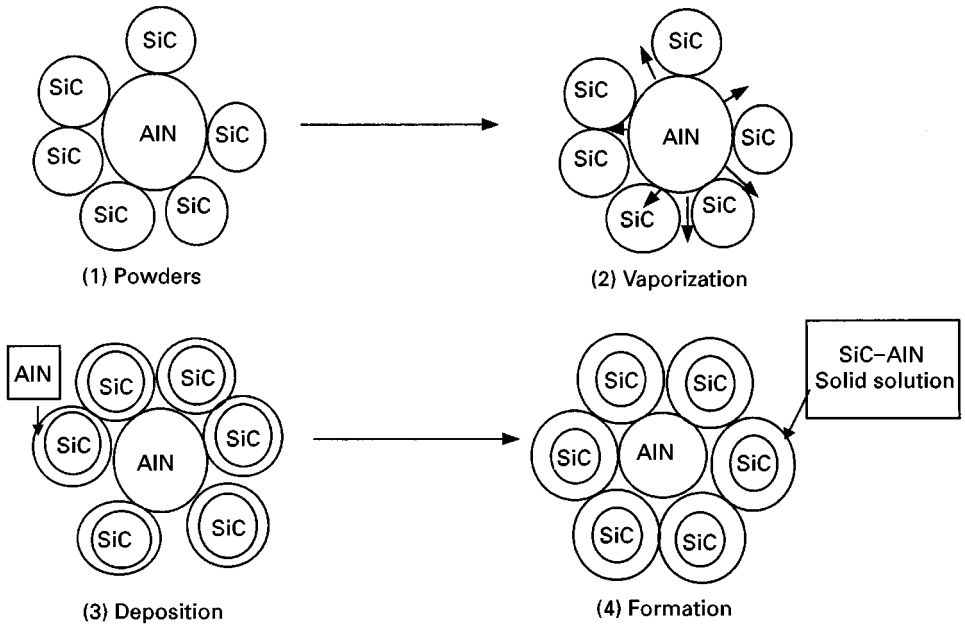

Figure 4 A schematic illustration of the solid-solution mechanism in the SiC–AlN composite system.

According to X-ray photoemission spectroscopy (XPS) analysis of the surface of the SiC–AlN composite, the diffraction peaks of 2θ angle for SiC and AlN are overlapped at 35° and 60° [6]. The average grain size of the SiC–AlN composite is 1 μm, as shown in the micrograph of Fig. 2. However, the original powder size of the AlN powder is about 3 μm. Therefore, the dispersed AlN particles must be changed in the fabrication process.

The solid vaporization pressures of AlN and SiC are 14 and 1.23×10^{-3} mm Hg at 1900 °C [7]. Of course, the vaporization rate of AlN solid far exceeds that of SiC at 1950 °C. It is imagined that the microstructure changes during the sintering process, as schematically shown in Fig. 4.

First, the second-phase particles, AlN, vaporize from the large powder surface, then AlN is deposited on the surface of the SiC powders, thus decreasing in size. Subsequently, AlN on the SiC surface diffuses into the SiC grain body, and finally SiC and AlN form an SiC–AlN solid solution layer on the surface of SiC grains. This formation mechanism may be proved by TEM analysis of the grain boundary shown in Fig. 5. Points 1,2,3 on the micrographs indicate the crystal boundary, the SiC grain near the boundary; and an SiC grain, respectively. Their diffraction peaks are shown in Fig. 6b–d, respectively. The silicon is basically constant from positions 1 to 3, but the aluminum decreases, and is especially lacking in the SiC grains, such as at position 3. Because the sintering process was conducted for only half an hour, the AlN may incompletely diffuse into the SiC grains, and form a solid solution with SiC; thus the microstructure is not affected during the formation of the homogeneous structure of the SiC–AlN solid solution.

3.2. The mechanisms of toughening and reinforcement

The presence of thermal residual stresses may cause microcracks to develop near the crack tip. The toughness could be increased, not only by the presence of microcracks, but also possibly due to preferential crack deflection towards microcrack regions. Theoretically, the largest contributions are predicted to be from crack deflection around the particles and from thermal residual stresses. The crack deflection around the particles must make a significant contribution to the toughness of the composite. Other additional contributions to toughness from particulate reinforcement potentially come from matrix grain-size reduction. It is therefore deduced that the toughening observed derives principally from a favourable residual stress distribution generated by the thermal expansion mismatch between the SiC matrix and AlN particles.

In order to make precise observation of the crack propagation and the crystal boundary, the surface of the SiC-AlN composite was diamond polished in decreasing grades from coarse to fine. To make the boundary clear, the sample was corroded by an alkali solution. The SiC–AlN specimen, shows crack deflection and bowing, as shown in Fig. 6. The crack extension path is curved and long, so that the damage requires more energy. The result would be an increase in the fracture toughness of the SiC–AlN composite, and as a result the fracture toughness reaches 7.01 MPa $m^{1/2}$. At the same time, the aluminium nitride exists at the interface between the SiC grains and forms a solid solution with SiC. The solid solution structure around the SiC grains restrains the exceeding growth of SiC crystal grains which became fine, as shown in Fig. 3. Owing to this behaviour, the bending strength of the SiC–AlN composite reaches 800 MPa at room temperature.

3.3. The mechanical properties of SiC–AlN composite

The results of the above analysis show that AlN may be deposited on the SiC surface and form a solid

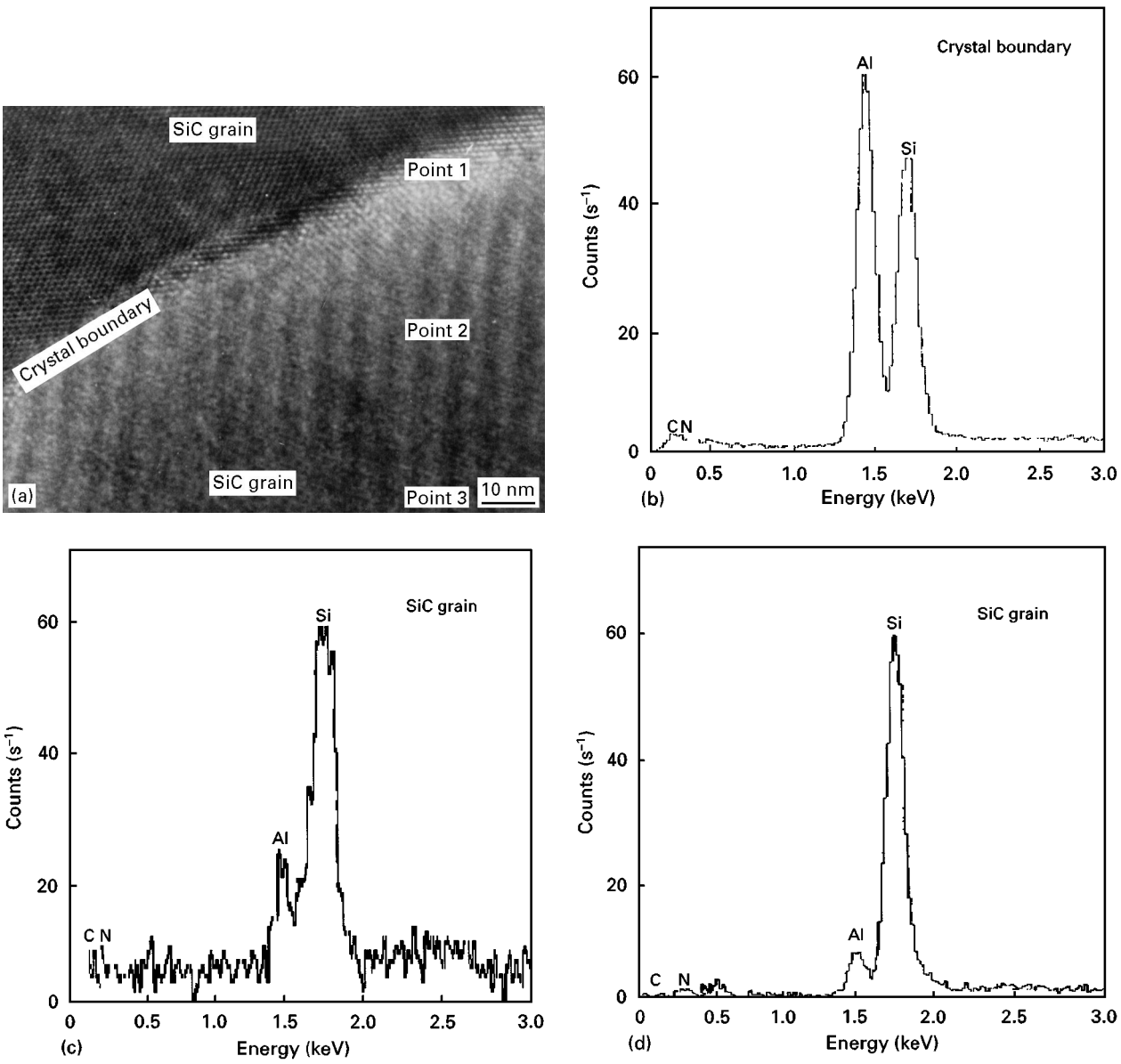

Figure 5 The crystal boundary of SiC–AlN and Al/Si elements. (a) TEM image of the microstructure of the crystal boundary. (b) The Al/Si diffraction peaks at point 1. (c) The Al/Si diffraction peaks at point 2. (d) The Al/Si diffraction peaks at point 3.

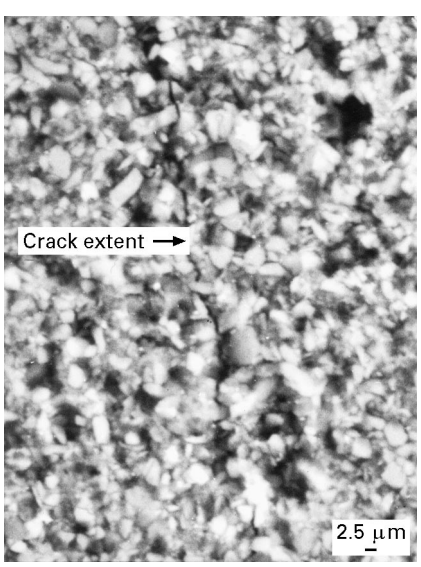

Figure 6. Crack propagation on the surface of the SiC–AlN composite.

solution, the boundary of which produces a barrier to restrain the excessive growth of the SiC grains. Therefore, this composite material shows fine microstructure and better mechanical properties.

The composition in this investigation was SiC: AlN: Y_2O_3 = 85:14.5:0.5 (wt %). The SiC–AlN ceramic composite could be sintered to dense specimens by hot pressing under 40 MPa at 1950 °C in an argon atmosphere. The physical and mechanical properties of the composite are shown in Table II.

4. Conclusion

The fracture toughness results indicate that there is significant toughening due to the addition of AlN particles to an SiC matrix at room temperature. The SiC–AlN composite shows better mechanical properties. The bending strength is 800 and 640 MPa at room temperature and 1400 °C, respectively. The fracture toughness reaches 7.01 MPa m$^{1/2}$ at room

TABLE II The properties of SiC–AlN composite

Composition	Density	Porosity	Bending strength (MPa)		Fracture toughness
$SiC:AlN:Y_2O_3$	(g/cm^{-3})	(%)	RT	1400 °C	($MPa\,m^{1/2}$)
85:14.5:0.5	3.22	5.6×10^{-3}	800	640	7.01

temperature. AlN plays an extremely important role in the composite system. During sintering by hot pressing, solid-phase vaporization occurs on the surface of the AlN powders, and AlN deposits around the SiC grains, and the formation of solid solution for SiC and AlN finally occurs. For these reasons, the solid solution layer of SiC–AlN on the grain surfaces restrains excessive growth in SiC crystal grains and forms a fine microstructure. The results for both fine crystal grains and crack deflection may contribute to reinforcement and toughening in the SiC–AlN composite.

Acknowledgements

The authors thank Dr Makoto Kawagoe for valuable discussions, and also Mrs Megumi Nomiya for her assistance in the SEM operation.

References

1. B. CUTLER and P. D. MILLER, CO4B35/52 CO4B35/58, US Pat. 4141 740 (1979).
2. I. V. INTERRANCE, US AD-A206998 (1989).
3. S. YOSHIYUJI, I. S. KEN, HIROYUBI *et al. J. Mater. Sci. Lett.* **7** (1988) 795.
4. R. J. OSCROFT and P. T. DEREK, *J. Am. Ceram. Soc.* **75** (1991) 2327.
5. J. C. TERENCE and E. J. ROBERT, CO4B35/64 US Pat. 4687 657 (1986).
6. Y. B. PAN, S. H. TAN and D. L. JIANG, *Ceram. Trans. Adv. Ceram. Matrix Compos. II* **6** (1995) 297.
7. T. B. CAMCOHOB, "Handbook of High-melting Point Compound" (China Industry Publish Society, 1965).

Received 29 April
and accepted 24 September 1997